

# TESTING THINNED, BACKSIDE ILLUMINATED CCD AREA IMAGE SENSORS

George Root

Jet Propulsion Laboratory  
Pasadena, California

## ABSTRACT

During the last two years, Texas Instruments, Inc., has, with support from NASA, developed thinned, backside illuminated CCD area image sensors. Arrays of 100 x 160 and 400 x 400 elements have been produced. During this time a facility to test and evaluate these sensors has been assembled at JPL. For a typical space application the CCD sensor will be cooled, exposure will be controlled by a shutter and the video signal will be read-out at a slow rate compatible with spacecraft data systems. This mode of operation enhances some of the performance parameters of the CCD but also causes problems in device testing primarily due to the long frame times involved. In order to overcome these difficulties some novel test techniques have been developed making use of computer processing of the video data. This paper presents the results of testing device noise and nonuniformity. Read-out noise levels of 25-50 electrons rms and uncorrected nonuniformity of response of about 1-3% have been measured. A simple technique for linearly correcting nonuniformity is described and examples given. The technique is shown to be successful in reducing nonuniformity to the level of random noise.

## I. INTRODUCTION

During the last two years Texas Instruments, Inc., with support from NASA, has developed thinned, backside illuminated CCD area image sensors. The design and fabrication of these sensors has been described (Ref. 1 and 2) and will not be repeated here except to note that arrays of 100 x 160 picture elements (pixels) and 400 x 400 elements have been produced. Figure 1 is a photo of the "front side" of a 400 x 400 array. The "back side" of the silicon substrate is etched until the thickness of the active area is approximately 10  $\mu$ m. The image to be sensed is focussed on the thinned "backside" eliminating losses and interference effects caused by light passing through the "frontside" gate structure. Examples of some astronomical images taken using a 400 x 400 array are presented in another paper in these proceedings (Ref. 3).

For a typical space imaging application the CCD sensor will be cooled to reduce dark current, the exposure will be controlled by a shutter, and the video signal will be read-out at a slow rate compatible with spacecraft data systems. This mode of operation has at least two advantages in sensor performance. Since the exposure is controlled by a shutter, it is not necessary to reserve part of the sensor area for an opaque buffer, the entire array can be used for imaging. The second advantage stems from the slow read-out rate. It will be shown later that the slow read-out permits low noise operation of the on-chip precharge amplifier. However, the operating mode described also causes some problems in device testing. A means for cooling the sensor must be provided,

and the test procedures must take into account the long frame times caused by slow read-out. At a typical rate of 100 k pixel/sec it takes 1.6 seconds to read out a 400 x 400 element image.

Figure 2 is a photo of the CCD test facility developed at JPL. The CCD sensor is mounted within a double walled vacuum dewar where it is cooled to a temperature in the range -40°C to -90°C by circulating cold nitrogen gas which is boiled off from a dewar of liquid nitrogen. The video data read-out from the CCD is amplified and digitized to 12 bit accuracy. This digital data is recorded on magnetic tape for subsequent computer processing. High resolution video monitors can be used to observe the data coming directly from the CCD in real time or to display data read back from digital tapes after computer processing.

This paper will describe some of the results of tests to measure the noise and nonuniformity associated with these CCD sensors, and a simple but effective method for removing nonuniformity in order to achieve noise limited performance.

## II. NOISE

The Texas Instruments' CCDs incorporate an on-chip precharge amplifier. An off-chip correlated double sampler is used to reduce the reset noise associated with this type of preamplifier which would otherwise amount to some 200 electrons rms. Figure 3 shows the results of a theoretical analysis of the minimum possible noise for this type of signal extraction technique. Only two sources of noise were considered in this analysis, thermal noise associated with the "off" resistance of the on-chip FET reset switch,  $R_{OFF}$ , and thermal noise associated with an equivalent noise resistance,  $R_N$ , representing the actual load resistor combined with "white" noise generators in the output source follower and the input stage of the off chip amplifier, all divided by the gain of the source follower squared. As shown, the output noise is a function not only of the parameters  $R_{OFF}$  and  $R_N$ , but also on the time between the samples of the reset voltage (clamp) and the signal voltage (sample). It is assumed that as the time between the clamp and the sample is varied, the bandwidth of the signal chain is correspondingly changed to retain optimum performance. The optimum relationship between clamp to sample time and video bandwidth is indicated by the two scales at the bottom of the figure. The curves of Figure 3 indicated that very low values of read out noise can be achieved with this type of amplifier, but only if  $R_{OFF}$  is large,  $R_N$  is small, and the time between clamp and sample can be made relatively large, say in the range of 1  $\mu$ s to 10  $\mu$ s. Since a typical spacecraft data system would require a relatively slow read out rate anyway, the performance of this type of signal chain is nicely matched to the requirements. Although the TI CCDs have been operated at read out rates of several million pixels per second,

noise measurements at JPL have all been done at a rate of 100 K pixel/sec and with a clamp to sample time of 2  $\mu$ s. The vertical bar near the center of Figure 3 indicates the range of readout noise measured for current CCDs using buried channel source follower FETs, 25 to 50 electrons rms. Earlier CCDs with surface channel FETs exhibited noise levels of about 100 electrons rms.

One common technique for measuring the noise of CCDs is to sample the output of a single pixel on successive frames and to measure the standard deviation of a large set of such samples. This technique is not suitable for slow read out rates; at 100 K pixel/sec it would take nearly 3 minutes to collect 100 samples. Any drift in lamp output or irregularities in exposure time during this period would be measured as noise. A more accurate as well as faster technique is made possible by computer processing of the recorded video data. To measure the output noise at any exposure level, two consecutive frames taken about 2 seconds apart are recorded. A small area, typically 20 pixels square is selected from both frames and the difference between output levels is taken on a pixel by pixel basis. The mean value of these 400 differences is near zero and is an indication of the drift in the system during the 2 seconds between frames. This mean difference is largely due to slight variations in exposure time and is ignored. However, the standard deviation of the 400 differences is just  $\sqrt{2}$  times the noise in either of the frames, assuming the noise is uncorrelated frame-to-frame. Since the differences are taken pixel by pixel, nonuniformity in output from pixel to pixel does not appear in the measured noise. Figure 4 is a typical plot of noise versus output measured by this technique. This particular curve is for a 400 x 400 array identified as JPL 12. At high output levels the measured noise tends toward shot noise in the output as would be expected, confirming the validity of the technique. It should be noticed that this technique does not respond to low frequency noise components which effect primarily the mean value of the differences rather than their variance.

To demonstrate the low noise capabilities of these CCDs, the series of photos in Figure 5 were made. The area shown is a portion of the same 400 x 400 array whose measured noise is shown in Figure 4. The photos are of raw video without processing and each photo is a single exposure. The peak signal level for the brightest bars is shown below each photo. Nonuniformity in response causes the signal level near the top and bottom of the array to be less than shown. Light and dark bands running horizontally across the photos are 60 Hz pickup. Since the full well capacity of this CCD is over  $3 \times 10^5$  elec/pixel, the 50 electron photo represents a sensor dynamic range of over 6000. Figure 5 demonstrates that quite usable images are possible with these sensors with only a few hundred electrons of signal. Combined with the high quantum efficiencies possible with "backside" illumination this results in a very useful low light sensor.

The photos in Figure 5 demonstrate low signal performance where, for cooled sensors, performance is limited by temporal noise. At high signal levels, however, performance is limited by

pixel to pixel nonuniformity in response. This will be discussed in the next section.

### III. NONUNIFORMITY

CCD image sensors, as do all discrete photo sensor arrays, exhibit pixel to pixel variation or nonuniformity of response. Figure 6 shows computer generated pseudo-three-dimensional plots of sensor output for dark and uniform illumination at 700 nm for a 100 x 160 element CCD identified as JPL 10. Note the 4X difference in scale factors for the two plots. The unit DN is just the digital number the A/D converter assigns to each pixel's output. In the dark plot, except for the blemish in the lower right corner, the variations visible are due to random temporal noise, that is if the same test were done again the pattern would be different. However, for the illuminated case the variations are large compared to the noise and are quite repeatable. These plots show good uniformity of response across the array which indicates a uniformly thinned sensor. Current 400 x 400 arrays exhibit more large scale variation in response associated with variation in the thickness of the finished sensor. The measured pixel to pixel nonuniformity is about the same for both sensor sizes.

The pixel to pixel sensor nonuniformity is measured by calculating the standard deviation of outputs for a uniform exposure for a small area, again typically 20 x 20 pixels. Figure 7 is a plot of the results of such a nonuniformity test on the same sensor as shown in Figure 6. As can be seen the output nonuniformity increases in direct proportion to the output. The proportionality constant, the slope of the line, is a measure of response nonuniformity, in this case  $\pm 2.6\%$ . The zero response, i. e. dark, intercept is a measure of dark nonuniformity, in this case  $\pm 97$  electrons. This is an older device with a measured noise of about 100 electrons rms again indicating that at low temperatures variations in dark output are due to temporal noise.

The plot in Figure 7 demonstrates the problem of achieving noise limited performance at high signal levels. For example, at an output of  $10^5$  electrons, Figure 7 shows a nonuniformity of about  $\pm 3000$  electrons/pixel. Referring back to Figure 4 it is seen that the noise at this output level is only about 300 electrons, so to achieve noise limited performance requires the removal or correction of a nonuniformity about 10 times larger than the noise. A simple technique for accomplishing this will be discussed next.

### IV. NONUNIFORMITY CORRECTION

Measurements of the linearity of CCD and signal chain have shown them to respond linearly within the resolution limit imposed by the 12 bit A/D converter. Since this is true, the response of each individual pixel can be characterized by two parameters indicating the slope and offset of that pixel's light transfer curve. Those two parameters can be measured by using uniformly illuminated calibration frames. In order to reduce the uncertainty in the calibration coefficients, each calibration frame is repeated several times,

typically four times, and the results averaged pixel by pixel. For each pixel a least mean squares straight line fit of the form  $y = a + bx$  is made using the averaged data where  $y =$  the individual pixel's output and  $x =$  the mean output of all pixels. The coefficients  $a$  and  $b$  are such as to correct each individual pixel's response to be equal to the average of all pixels. The set of coefficients,  $a$  and  $b$ , represents the calibration data. At some later time a set of raw image data can be corrected using the relationship (corrected data) = (raw data -  $a$ )/ $b$ . To assess the efficacy of this correction, the standard deviation of the corrected data is found and compared to the standard deviation of the raw data, and to be random noise level. A "perfect" correction would be indicated by a standard deviation equal to about 1.12 times the random noise, i. e. the rms sum of the noise in the data and the residual noise in the calibration coefficients. This could supposedly be reduced to just the random noise by repeating each calibration frame more than four times.

Figure 8 shows the results of such a test using an area of 30 x 30 pixels. Again a partial area is used to reduce processing cost, and in this case to eliminate blemishes from the area tested. A 700 nm spectral filter was used to prevent spectral shifts as the lamp intensity was varied. The standard deviation of the raw data is similar to that shown in Figure 7, again indicating an uncorrected nonuniformity of about  $\pm 2.8\%$ . The standard deviation of the linearly corrected data is slightly above the random noise level as expected indicating that simple linear correction is quite effective in reducing output nonuniformity. In fact, the rightmost data point shows a residual nonuniformity of about  $\pm 5$  DN for an output signal of about 2500 DN or a residual error of  $\pm 0.2\%$ .

Figure 9 shows the results of using linear decalibration to correct response nonuniformity in a 100 x 160 pixel image. The contrast has been enhanced to accentuate the results, both photos have the same contrast enhancement. Most of the spots in the prints are due to chemical processing of the film and not the CCD. It should be noted that although this decalibration process removes nonuniformity of response, it does not change the signal to noise ratio and in the photos shown the S/N ratio is lower in the top left corner because that area of the array had lower sensitivity. It may be possible to see the slightly more "noisy" appearance of that area of the corrected photo.

In order for this technique of correcting sensor nonuniformity to be of practical usefulness, the pattern of nonuniformity must be stable and repeatable. To determine if this is the case, a one week stability test was conducted. The results are shown in Figure 10. The calibration data were taken at time  $t=0$  and then this single set of data were used to decalibrate test frames taken over a period of one week. The vertical axis is the residual dispersion in the data after being corrected as described above. The three curves are for dark output and two light levels corresponding to about half and one third of full well. It should be noted that the tests were done at room temperature to avoid problems of frost and dew collecting on the dewar windows. This accounts for the high level of dark output and dark noise. The three arrows at the right of the figure indicate the expected level of residual nonuniformity (1.12

times the random noise) expected for each curve. As can be seen the residual dispersion is again due essentially entirely to random noise, that is, the fixed nonuniformity pattern has been "completely" removed. These curves also show that the pattern of nonuniformity is stable over a period of at least one week within the level of random noise.

## V. MEMBRANE INTERFERENCE

When thinned CCD sensors are used to image in nearly monochromatic light, interference fringes are generated within the silicon membrane and are visible in the video output. This effect is noticeable only for wavelengths long enough that the light can make at least one double pass through the membrane ( $\lambda$  greater than about 600 nm) and for spectral bandwidths narrow enough to produce well defined fringes ( $\Delta\lambda$  less than about 50 Å). One application where this effect is apparent is methane band imaging at 890 nm. The index of refraction of silicon is so high, approximately 4, that light travels through the silicon essentially perpendicular to the surface regardless of incidence angle. Thus, at least to first order, the interference pattern generated in the silicon wafer is a function only of the thickness variation of the wafer and not of the incidence angle of the light, nor of the nature of the image focussed on the CCD surface. For a constant temperature, the thickness variations of the wafer should be fixed and so the interference pattern should appear to be another form of fixed pattern response nonuniformity which can be corrected using the technique described above. To test this hypothesis, a 100 x 160 element CCD was illuminated by tungsten light passed through an 890 nm methane band filter (half power bandwidth 40 Å). Figure 11 shows the results of this test. The left photo is the "flat field" containing the interference pattern used for decalibration. The image used is that of a medium contrast bar target. The peak to peak signal amplitude is about the same as the peak to peak amplitude of the interference pattern. Again the simple linear decalibration is quite effective in correcting for sensor response nonuniformity.

## REFERENCES

1. Antcliffe, G. A., L. J. Hornbeck, J. M., Younse, J. B. Barton, and D. R. Collins, "Large-Area CCD Imagers for Spacecraft Applications", Symposium on Charge-Coupled Device Technology for Scientific Imaging Applications, Pasadena, California, March 6-7, 1975.
2. Antcliffe, G. A., L. J. Hornbeck, W. C. Rhines, W. W. Chan, J. W. Walker, and D. R. Collins, "Development of a 400 x 400 Element, Backside Illuminated CCD Imager", 1975 International Conference on the Application of Charge-Coupled Devices, San Diego, California, October 29-31, 1975.
3. Smith, B. A., "Astronomical Imaging Applications for CCDs", Paper 5 of Session Five of these Proceedings.

Acknowledgment. This paper presents the results of one phase of research carried out at the Jet Propulsion Laboratory, California Institute of Technology, under Contract NAS7-100, sponsored by the National Aeronautics and Space Administration.

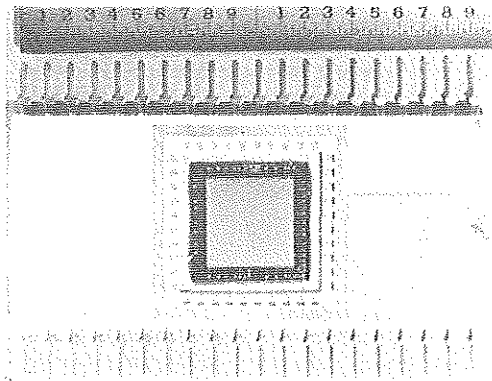


Figure 1. Texas Instruments 400 x 400 Element CCD Image Sensor



Figure 2. CCD Test Facility at JPL

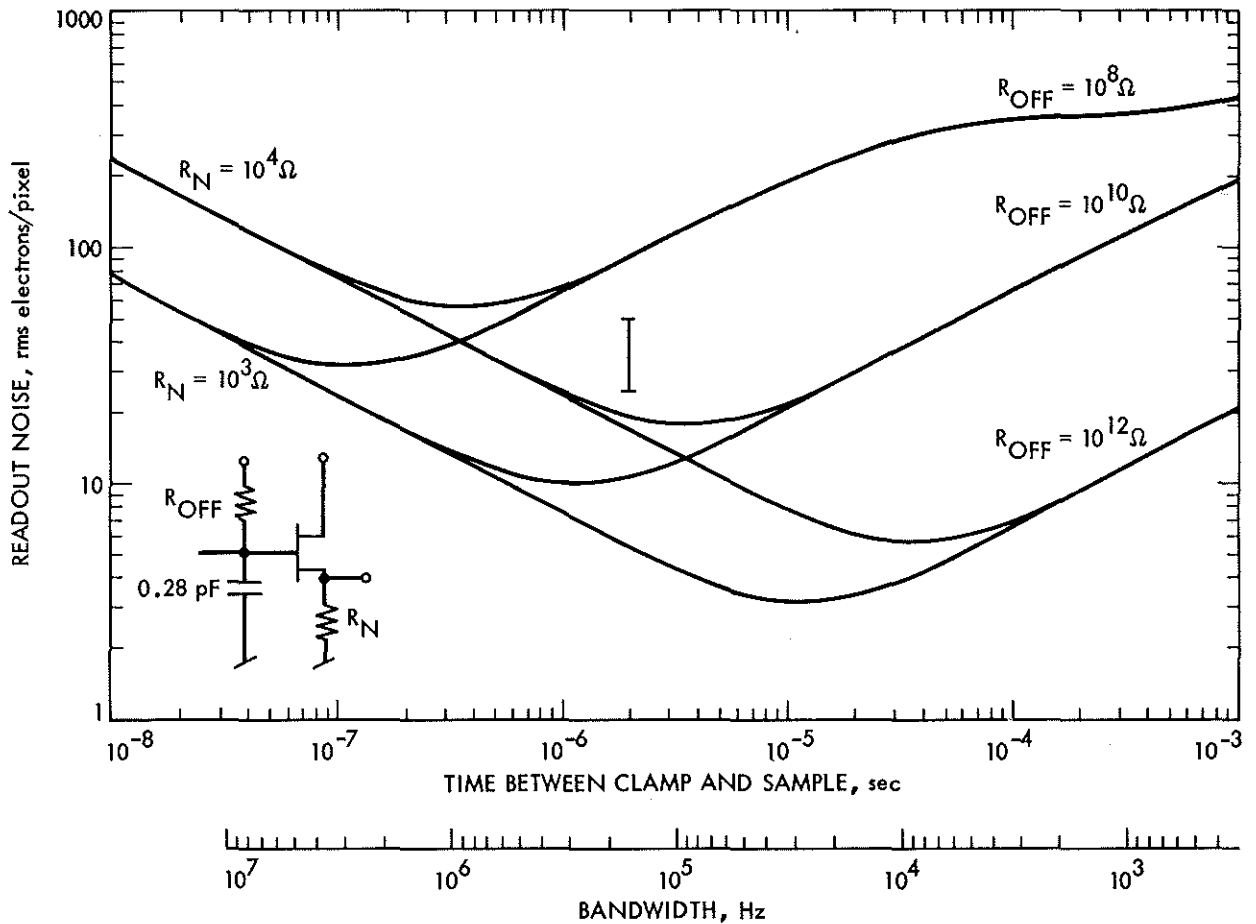


Figure 3. Minimum Read Out Noise for Precharge Amplifier-Correlated Double Sampler Combination

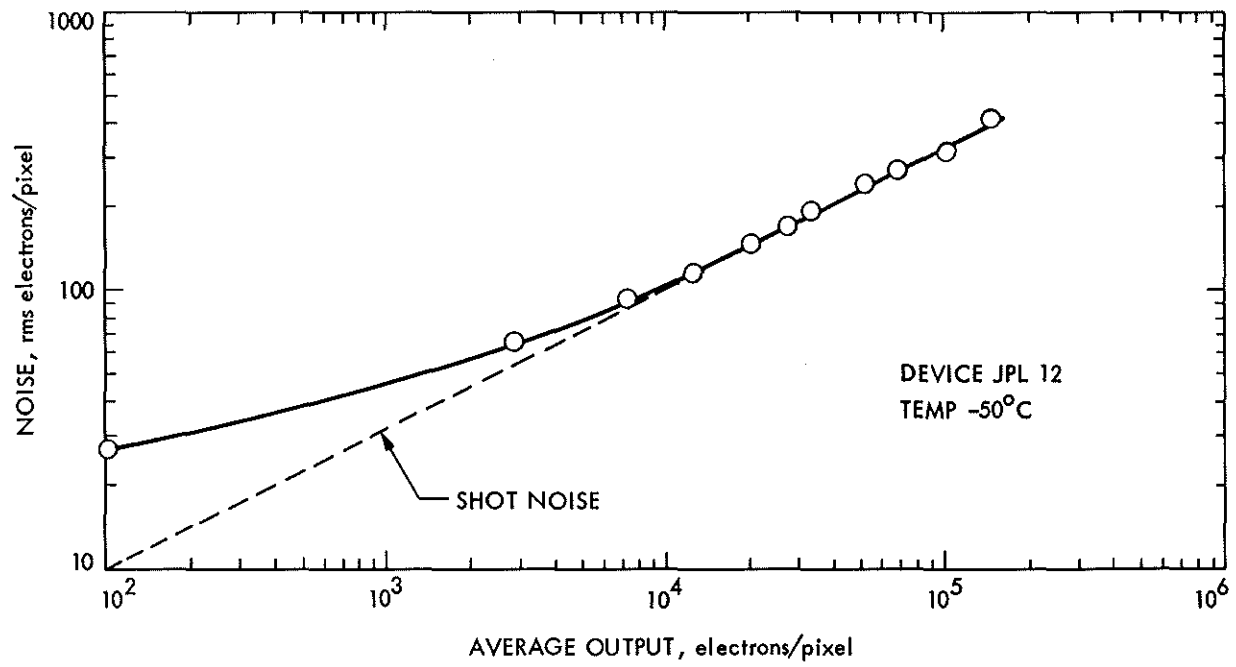


Figure 4. Measured Output Noise

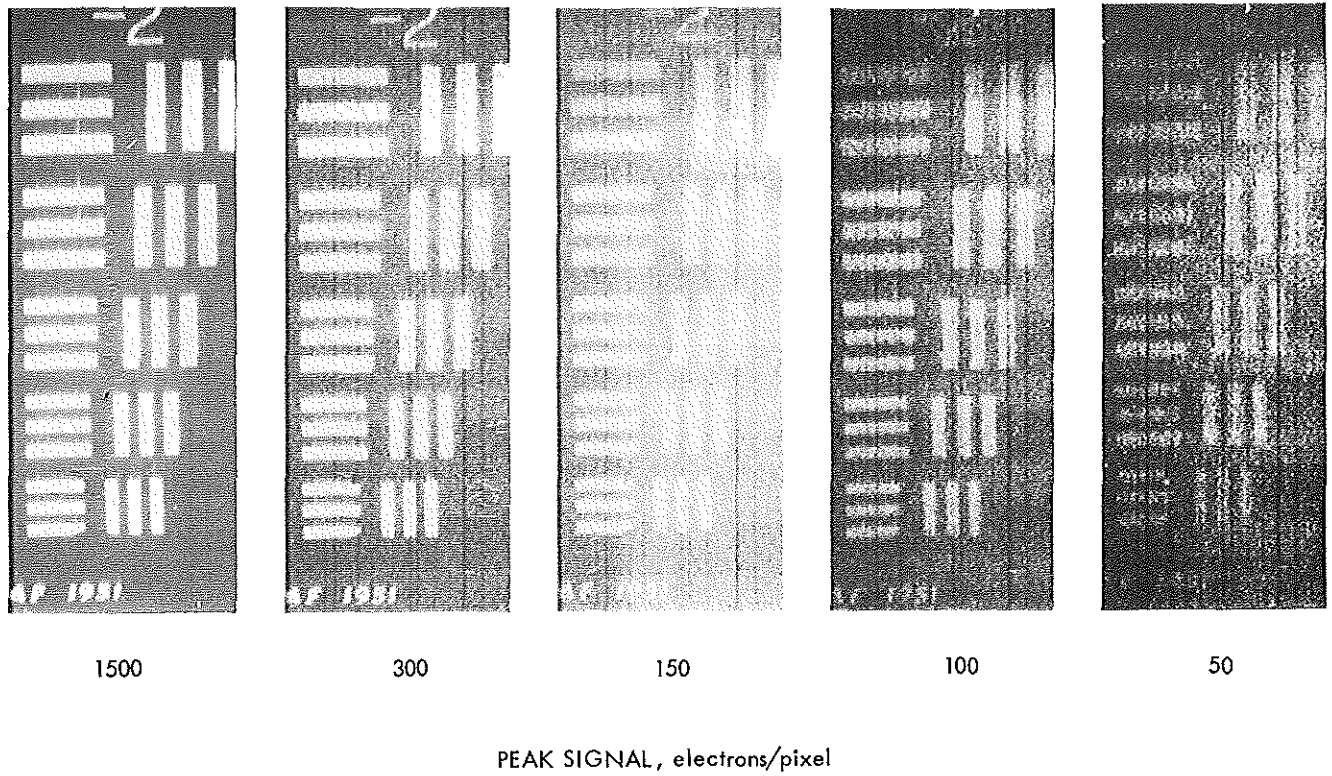


Figure 5. Examples of Low Light Level Images

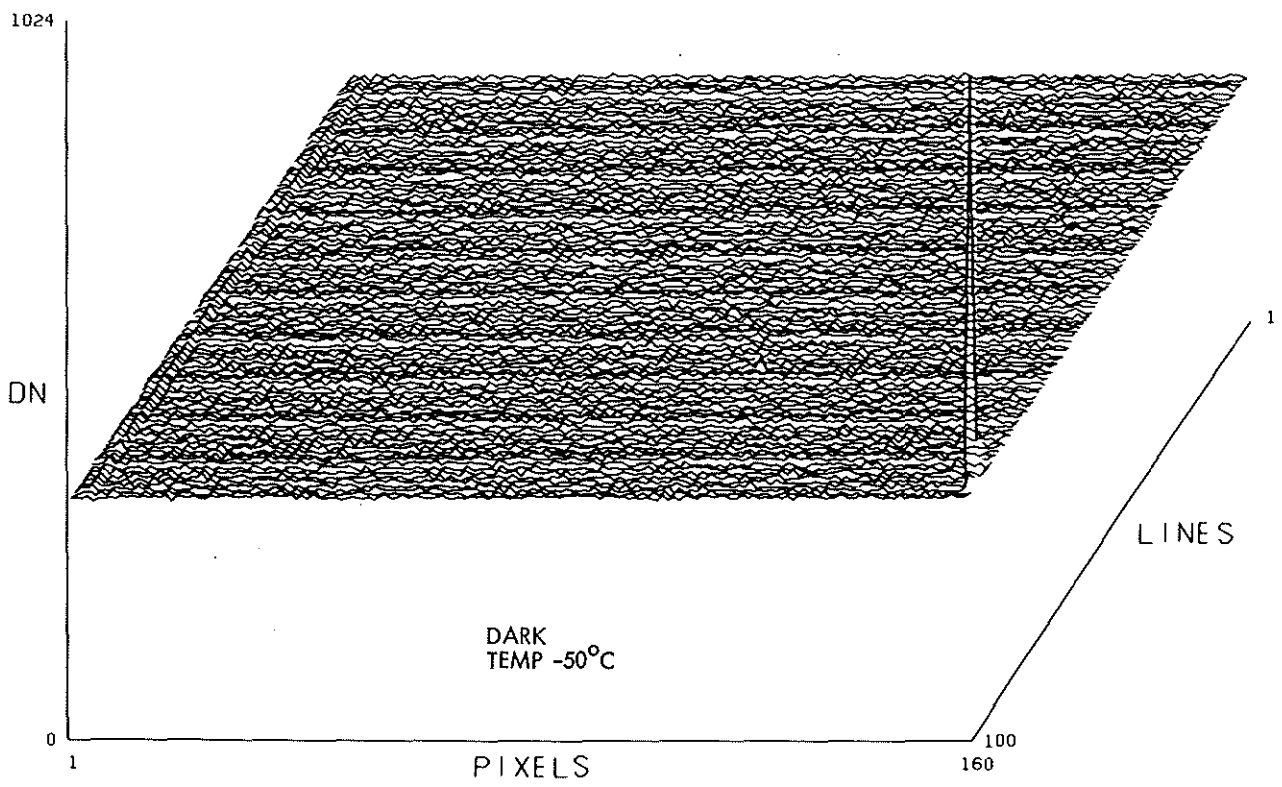
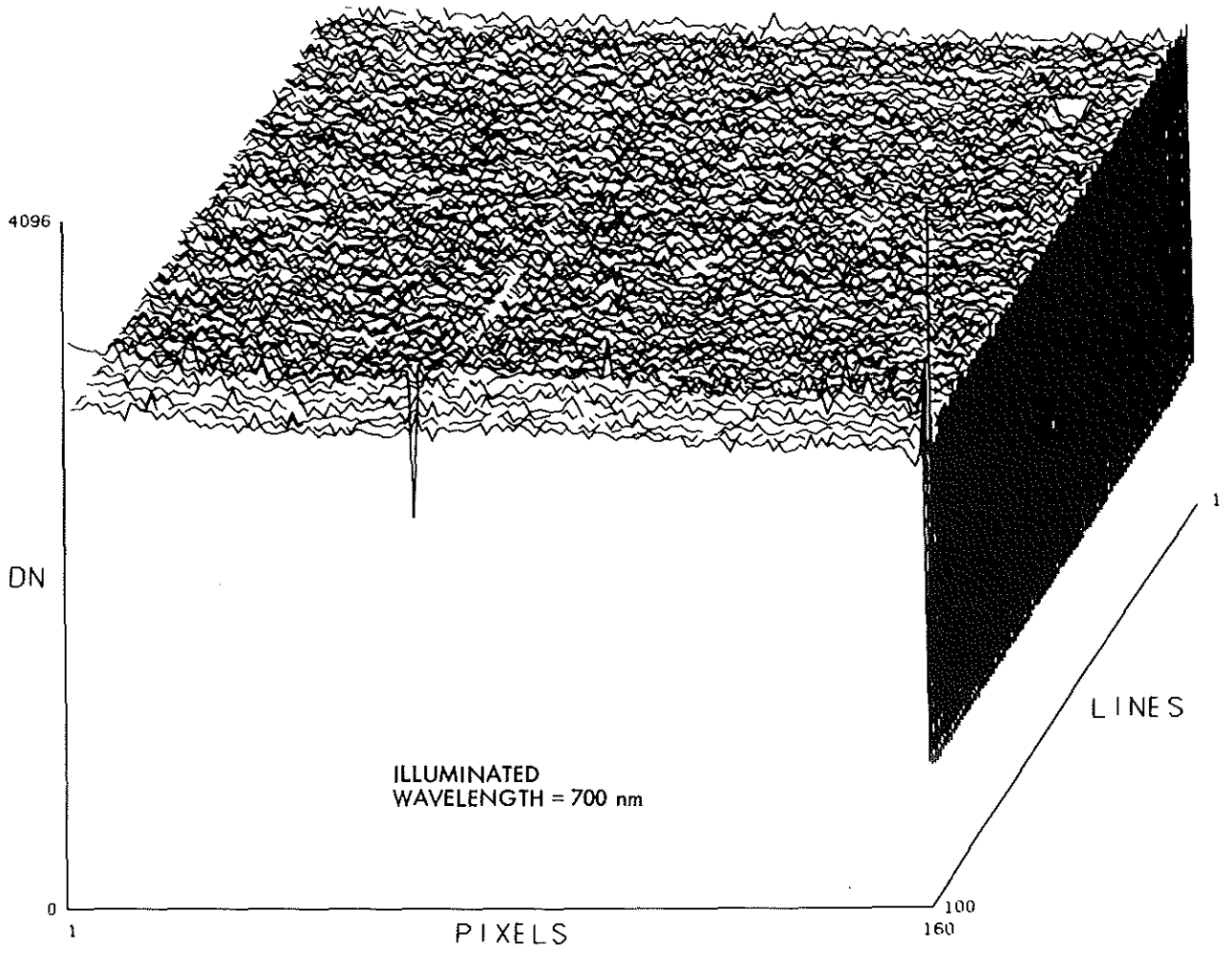


Figure 6. Computer Generated Plots of 100 x 160 Element CCD Output

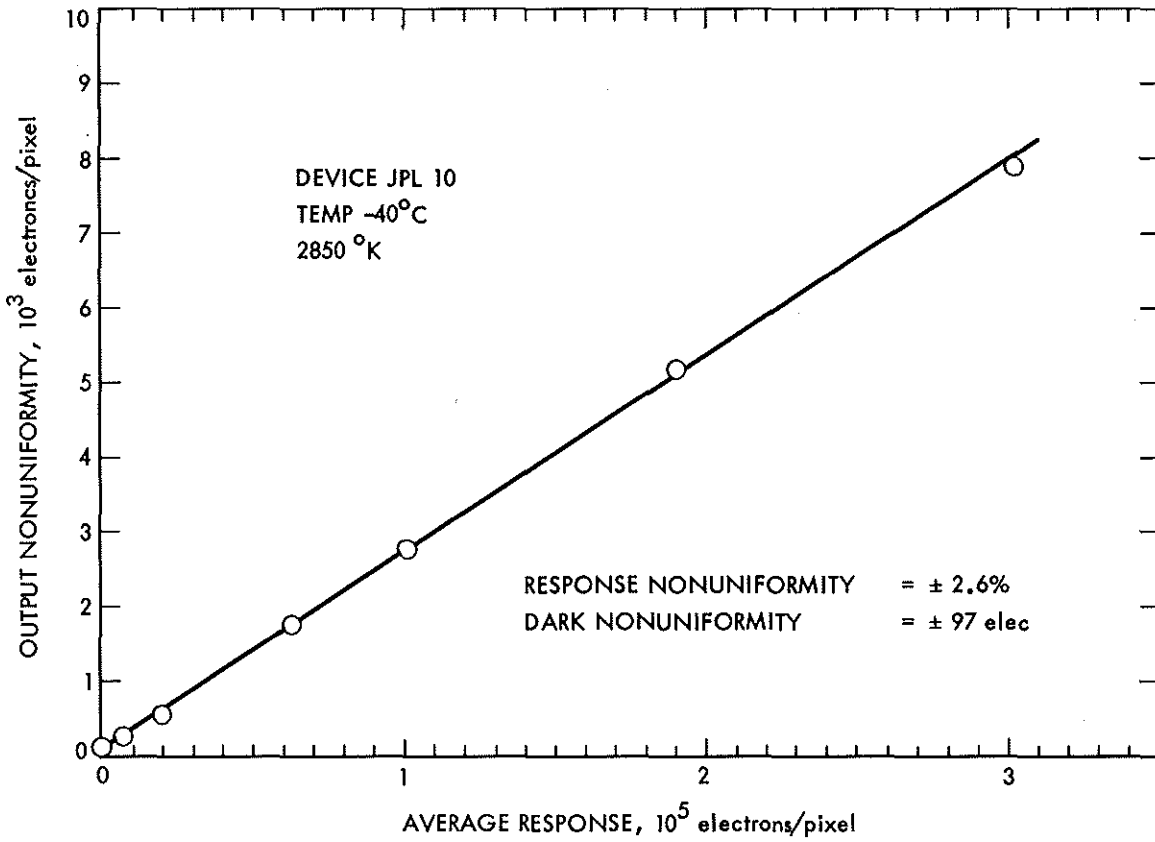


Figure 7. Measured Output Nonuniformity

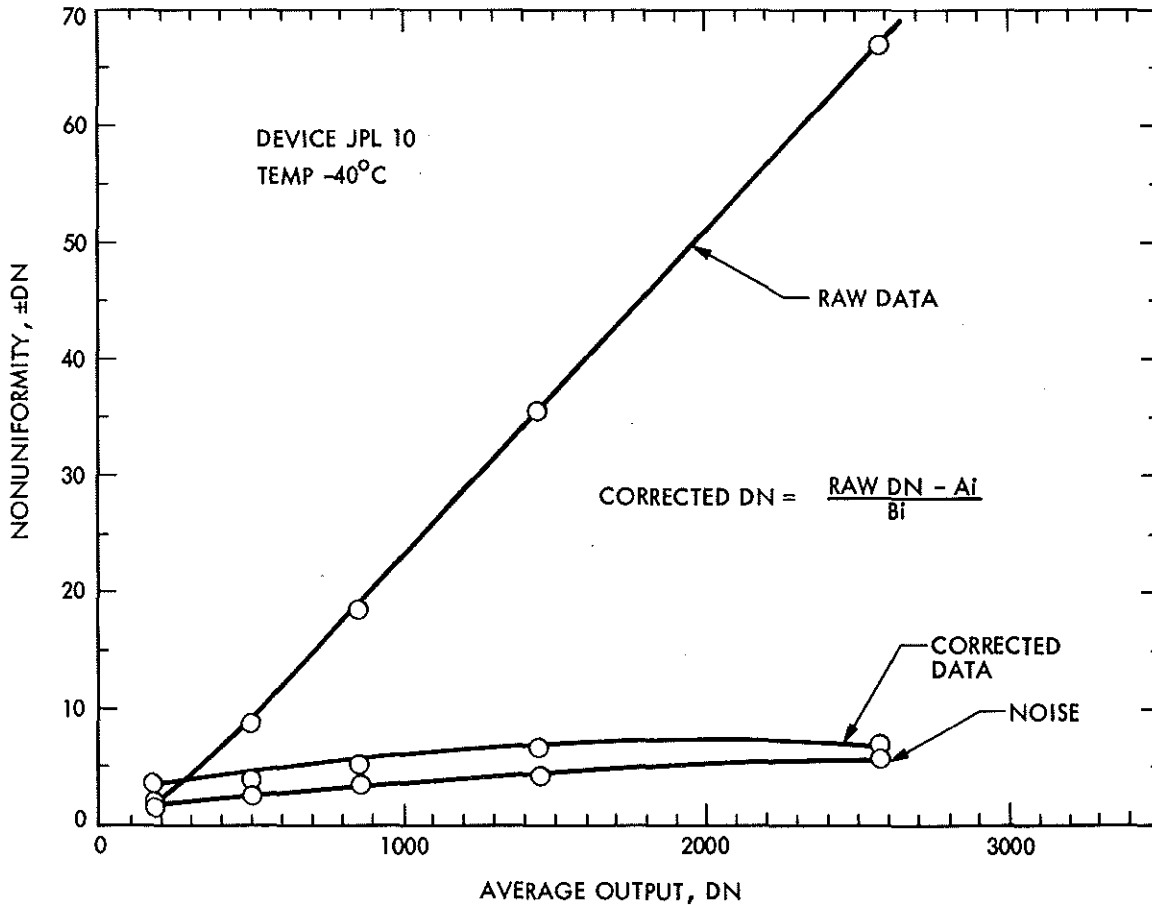


Figure 8. Nonuniformity of Raw Data and Linearly Corrected Data

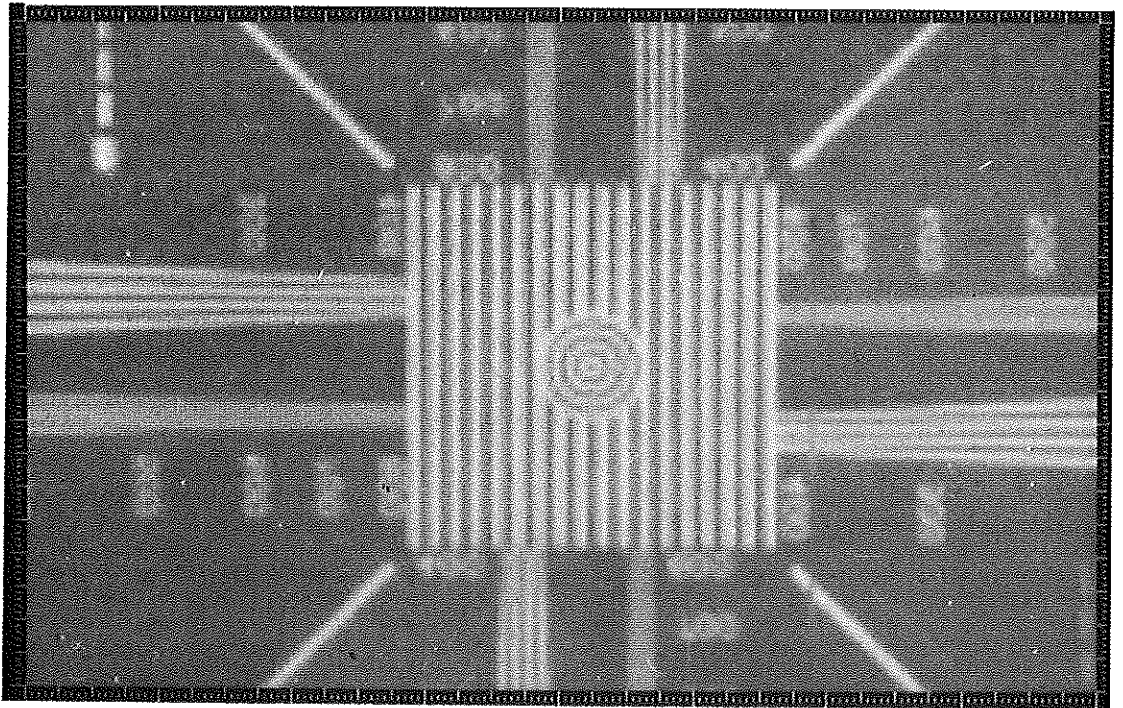
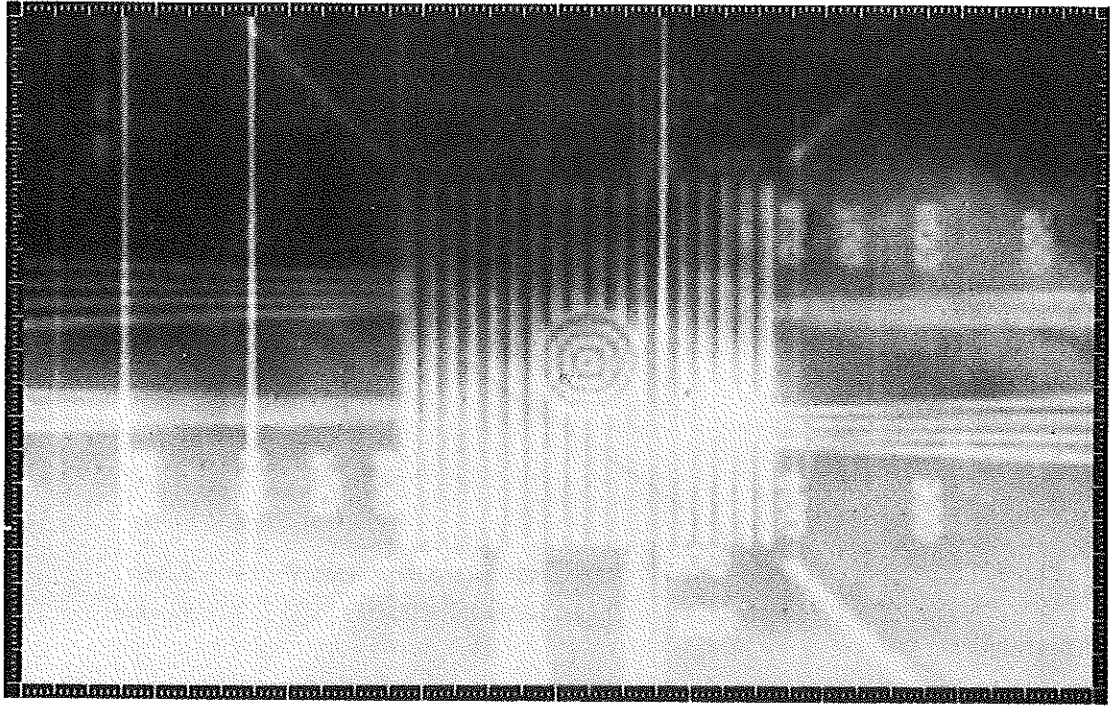


Figure 9. Raw and Corrected Images from 100 x 160 Element CCD



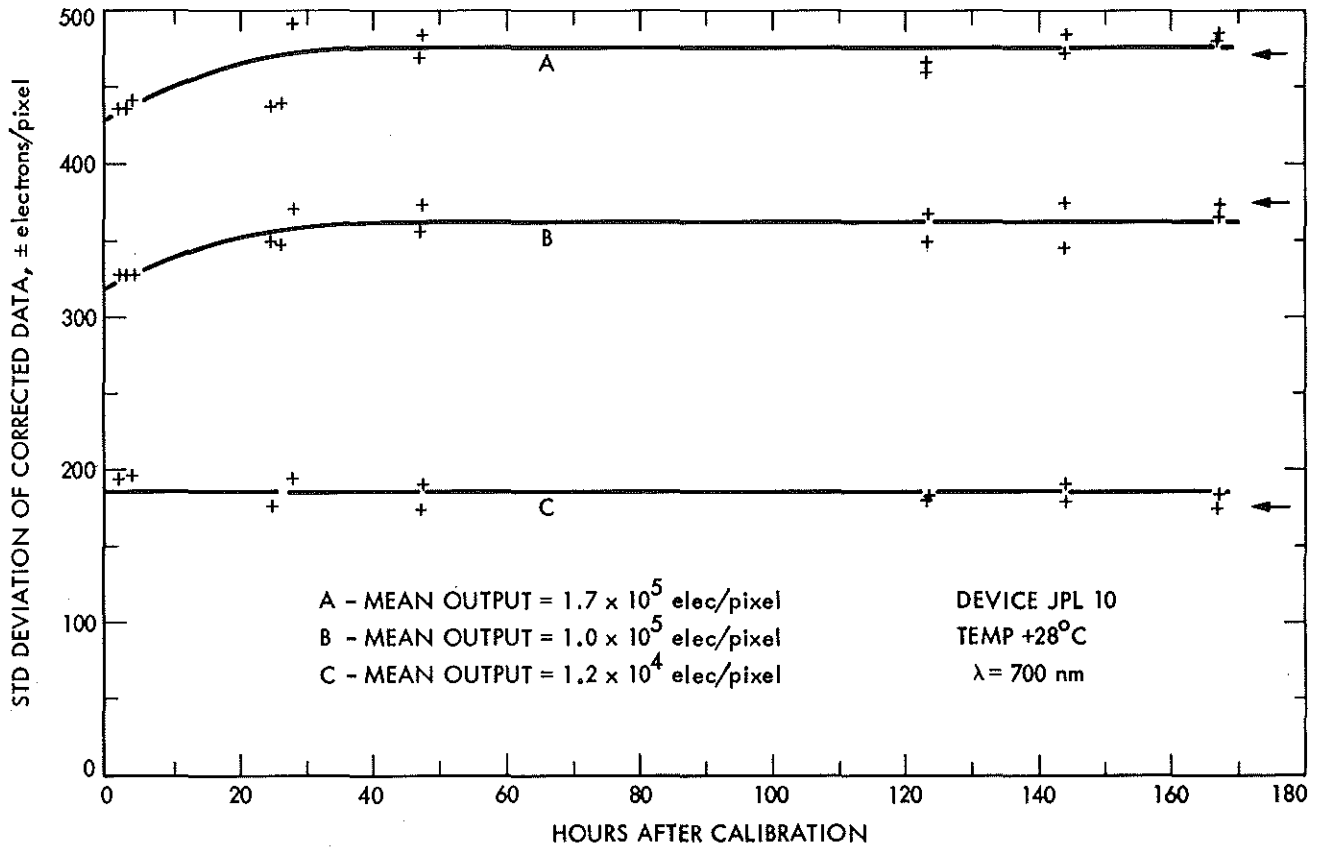


Figure 10. Stability of Nonuniformity Correction

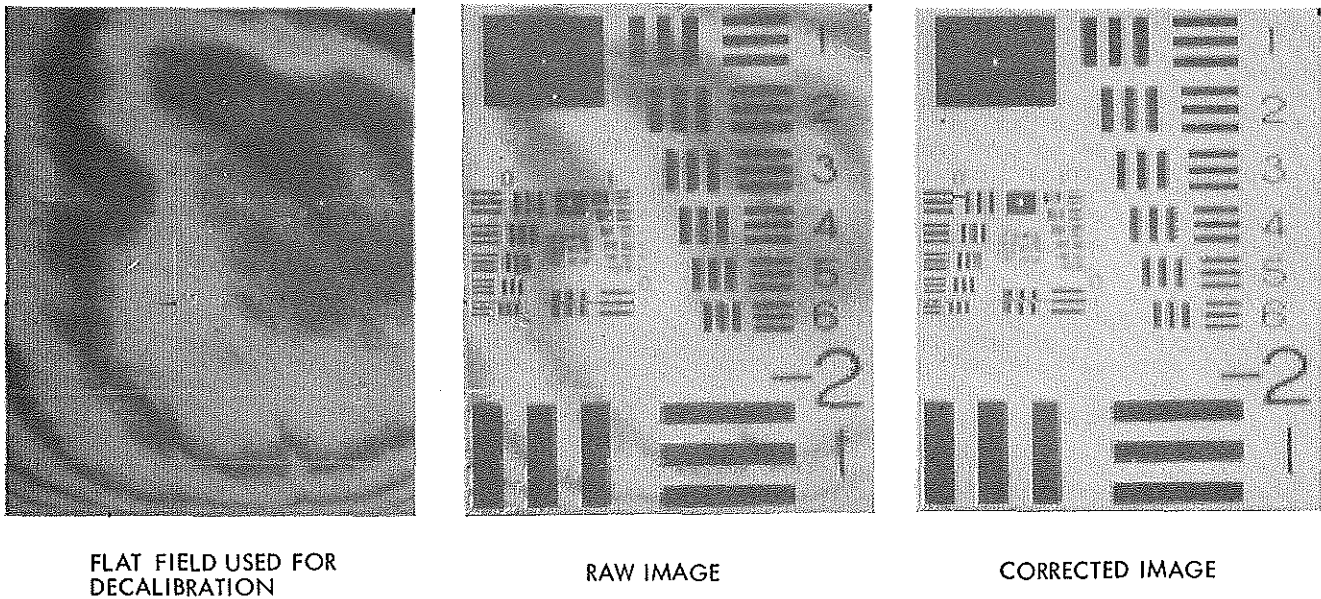


Figure 11. Correction of Interference Pattern Caused by Imaging through Narrow Band Filter at 8900 Å